doi:10.1016/j.jmb.2007.02.063 J. Mol. Biol. (2007) 368, 982–997

JMB

Available online at www.sciencedirect.com
ScienceDirect

ELSEVIER

β-Sheet Structured β-Amyloid(1-40) Perturbs Phosphatidylcholine Model Membranes

Maurits R. R. de Planque[1,2]*, Vincent Raussens[3] Sonia Antoranz Contera[2], Dirk T. S. Rijkers[4], Rob M. J. Liskamp[4] Jean-Marie Ruysschaert[3], John F. Ryan[2], Frances Separovic[5] and Anthony Watts[1]

[1]*Biomembrane Structure Unit Department of Biochemistry University of Oxford South Parks Road Oxford OX1 3QU, UK*

[2]*Clarendon Laboratory Department of Physics University of Oxford Parks Road, Oxford OX1 3PU, UK*

[3]*Laboratory for the Structure and Function of Biological Membranes, Free University of Brussels, B-1050 Brussels Belgium*

[4]*Department of Medicinal Chemistry and Chemical Biology, Utrecht University Sorbonnelaan 16, 3584 CA Utrecht, The Netherlands*

[5]*School of Chemistry Bio21 Institute, University of Melbourne, Melbourne VIC 3010, Australia*

**Corresponding author*

The disruption of intracellular calcium homeostasis plays a central role in the pathology of Alzheimer's disease, which is also characterized by accumulation of the amyloid-β peptides Aβ40 and Aβ42. These amphipathic peptides may become associated with neuronal membranes and affect their barrier function, resulting in the loss of calcium homeostasis. This suggestion has been extensively investigated by exposing protein-free model membranes, either vesicles or planar bilayers, to soluble Aβ. Primarily unstructured Aβ has been shown to undergo a membrane-induced conformational change to either primarily β-structure or helical structure, depending, among other factors, on the model membrane composition. Association of Aβ renders lipid bilayers permeable to ions but there is dispute whether this is due to the formation of discrete transmembrane ion channels of Aβ peptides, or to a non-specific perturbation of bilayer integrity by lipid head group-associated Aβ. Here, we have attempted incorporation of Aβ in the hydrophobic core of zwitterionic bilayers, the most simple model membrane system, by preparing proteoliposomes by hydration of a mixed film of Aβ peptides and phosphatidylcholine (PC) lipids. Despite the use of a solvent mixture in which Aβ40 and Aβ42 are almost entirely helical, the Aβ analogs were β-structured in the resulting vesicle dispersions. When Aβ40-containing vesicles were fused into a zwitterionic planar bilayer, the typical irregular "single channel-like" conductance of Aβ was observed. The maximum conductance increased with additional vesicle fusion, while still exhibiting single channel-like behavior. Supported bilayers formed from Aβ40/PC vesicles did not exhibit any channel-like topological features, but the bilayer destabilized in time. Aβ40 was present primarily as β-sheets in supported multilayers formed from the same vesicles. The combined observations argue for a non-specific perturbation of zwitterionic bilayers by surface association of small amphipathic Aβ40 assemblies.

Keywords: Alzheimer's disease; amyloid-β peptide; membranes; phosphatidylcholine; lipid bilayer perturbation

Abbreviations used: Aβ40, β-amyloid(1-40) peptide; Aβ42, β-amyloid(1-42) peptide; AD, Alzheimer's disease; SUV, small unilamellar vesicle; MLV, multilamellar vesicle; CD, circular dichroism; AFM, atomic force microscopy; ATR-FTIR, attenuated total reflection Fourier transform infrared; CSA, chemical shift anisotropy; EM, electron microscopy; TFA, trifluoroacetic acid; TFE, trifluoroethanol; HFP, hexafluoroisopropanol; PC, phosphatidylcholine; PE, phosphatidylethanolamine; PG, phosphatidylglycerol; PS, phosphatidylserine; POPC, 1-palmitoyl-2-oleoyl-*sn*-glycero-3-phosphatidylcholine; POPC-d_{31}, 1-palmitoyl(d_{31})-2-oleoyl-*sn*-glycero-3-phosphatidylcholine; POPE, 1-palmitoyl-2-oleoyl-*sn*-glycero-3-phosphatidylethanolamine; DOPC, 1,2-dioleoyl-*sn*-glycero-3-phosphatidylcholine; DMPC, 1,2-dimyristoyl-*sn*-glycero-3-phosphatidylcholine.

E-mail address of the corresponding author: m.deplanque1@physics.ox.ac.uk

Introduction

The amyloid-β peptides (Aβ) became implicated in the etiology of Alzheimer's disease (AD) when it was established that they are the main component of the cerebrovascular fibrillar deposits and extracellular neuritic plaques that are characteristic of this progressive neurodegenerative disorder.[1,2] It was originally proposed that these fibrillar Aβ deposits cause the various symptoms of AD observed during its early and progressed stages,[3] but mounting evidence indicates that smaller, soluble forms of Aβ are the primary neurotoxic species.[4–6]

The Aβ peptides are produced by proteolytic processing of amyloid precursor proteins. These abundant membrane proteins are cleaved in the middle of their transmembrane helix and also close to the membrane surface in their extracellular domain, resulting in peptides with a length of 39–43 residues.[7] It is generally assumed that these Aβ peptides are expelled from the membrane because the truncated transmembrane segment is, with ~12 hydrophobic residues, too short for stable association with the membrane hydrophobic core. But it has also been argued that a fraction of the processed peptides remain associated with the membrane as a transmembrane α-helix,[8] and complete expulsion of helical Aβ peptides from a lipid bilayer was not observed in recent molecular dynamics (MD) simulations.[9,10]

In vitro studies have shown that the pronounced amphipathicity of the Aβ analogs enables self-assembly in a variety of higher order structures. At concentrations above 15 μM the secondary structure of Aβ40 changes from predominantly unstructured, the conformational indicator of monomeric Aβ, to predominantly β-structure, indicating oligomerization.[11,12] Depending on the Aβ species and concentration and factors such as pH, ionic strength, and temperature, the oligomerization proceeds through increasingly larger soluble Aβ assemblies towards insoluble protofibrils and mature fibrils.[13–15] At a molecular level these consist of stacked parallel β-sheets (in the case of Aβ40 formed by residues 12–24 and 30–40) that are arranged at right angles to the fibril axis in a cross-β motif.[16,17] The structure of the various prefibrillar soluble assemblies is not known, but a high β-sheet content seems likely.[18,19]

It is not clear how these neurotoxic structures can assemble *in vivo* because even in AD patients the concentration of soluble Aβ appears to be orders of magnitude below the micromolar concentration threshold required for *in vitro* oligomerization.[20] However, since fibrillogenesis is facilitated once a small amount of aggregated material has been formed,[21,22] this problem translates into a search for (extra)cellular components that trigger the initial oligomerization event.[23,24] Many studies have addressed the possibility that soluble Aβ peptides are attracted to membrane surfaces, which could act as a two-dimensional template for the formation of amyloid nucleation seeds.[24,25] Membranes have also attracted attention because disruption of intracellular calcium homeostasis, which appears to play a central role in the pathogenesis of AD, probably results from membrane destabilization.[2,26] Soluble Aβ could (in) directly target endogenous calcium channels, insert itself into the membrane to form multimeric pores, and/or perturb the membrane non-specifically by surface association.

Amyloid–membrane interactions have been widely studied with protein-free vesicles or planar bilayers because these enable detailed characterization of Aβ with biophysical methods. The effect of exposing such model membranes to soluble Aβ depends primarily on the initial Aβ assembly state (which is determined by the sample preparation protocol) and the membrane composition, specifically the presence of anionic lipids and glycolipids.[27,28] In dispersions of negatively charged vesicles, unstructured monomeric Aβ adopts a certain amount of secondary structure, either β-structure or α-helix, depending on experimental conditions,[12,27–31] suggesting that a charged membrane surface attracts Aβ peptides.

Release of encapsulated dyes,[27,28] shifts of lipid head group ^{31}P NMR resonances,[32,33] changes in bilayer fluidity[34] and monolayer studies[35–37] indicate that the structured Aβ is indeed associated with these anionic membranes, and fibril growth has been imaged on supported bilayers of total brain lipid extract.[38] These observations point to a non-specific mechanism of membrane perturbation. However, evidence for amyloid channel formation has also been obtained. Exposure of anionic planar lipid bilayers to an aqueous solution of soluble Aβ results in "single channel-like" electrical activity,[39–42] and channel-like structures have been imaged on supported PC bilayers.[43–45] However, the initial oligomerization state in the latter studies is unclear. This is relevant because unlike monomeric Aβ, oligomeric Aβ can also bind to zwitterionic membranes and is clearly more disruptive to model membranes and cells.[34,46–48]

Here we have used the mixed film method, designed to incorporate hydrophobic helical peptides in bilayers,[49,50] to study the interaction of Aβ40 peptides with zwitterionic model membranes. A dry peptide-lipid mixed film was prepared from a solvent mixture in which the Aβ peptide is α-helical, but hydration of this film resulted in zwitterionic vesicles with predominantly β-structured Aβ. These proteoliposomes gave rise to the typical single channel like conductance of Aβ when fused into a zwitterionic planar bilayer, and formed unstable supported bilayers, without any topological features, on a mica template. Our combined observations are consistent with a non-specific membrane perturbation of small oligomeric assemblies of Aβ.

Results

Mixed films of Aβ40 and phosphatidylcholine

The mixed film method for incorporation of hydrophobic peptides in lipid bilayers requires that peptides and lipids are mixed on a molecular level prior to vesicle formation. The organic solvent, or solvent mixture, that is used to solubilize the lipids should, therefore, also enable peptide solubilization. Lyophilized Aβ40 peptide was pretreated with trifluoroacetic acid (TFA) to remove aggregation seeds (see Materials and Methods) and the solubility of the Aβ-TFA film in various phosphatidylcholine-compatible solvents[54,55] was assessed by circular dichroism (CD) spectroscopy. The CD spectrum of TFA-pretreated Aβ dissolved in trifluoroethanol (TFE), shown in Figure 1, is characterized by a cross-over point at 200.5 nm and two minima near 207 and 221 nm with a relatively high residual molar ellipticity of -52×10^3 and -43×10^3 deg cm^2 dmol^{-1}, respectively, indicating that the conformation of Aβ in this solvent is approximately 80% α-helix and 20% random coil and that the TFA-pretreated peptide readily solubilizes in TFE.[56]

The minima and cross-over point are shifted to lower wavelengths for TFA-pretreated Aβ dissolved in hexafluoroisopropanol (HFP), whereas there is a shift to higher wavelengths in the case of methanol and isopropanol. These lineshapes indicate that the average conformation of the Aβ peptides is ~50% α-helix and 50% random coil in HFP, ~80% α-helix and 20% β-sheet (and/or β-turn) in methanol, and ~60% α-helix and 40% β-sheet in isopropanol. The spectrum of Aβ in ethanol is characterized by a cross-over point at 206 nm and a single minimum around 220 nm, corresponding to approximately 90% β-structure and only ~10% α-helix.[56] The intensity of these four spectra is reduced with respect to the spectrum of Aβ in TFE, but non-helical structure elements give a less intense CD signal.[56]

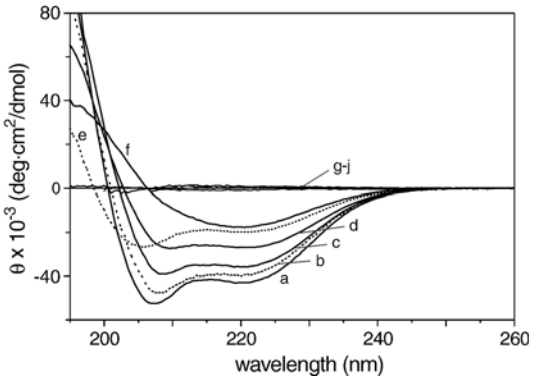

Figure 1. Circular dichroism spectra of TFA-pretreated Aβ40 in phosphatidylcholine-compatible organic solvents: (a) TFE, (b) TFE/methanol (2:1, v/v), (c) methanol, (d) isopropanol, (e) HFP, (f) ethanol, (g) hexane, (h) heptane, (i) decane, and (j) chloroform.

In contrast, the negligible spectral intensity (Figure 1) and the observed formation of particles in the case of heptane, hexane, decane, and chloroform, show that TFA-pretreated Aβ is insoluble in these solvents.

In the present study, the Aβ-PC mixed films were prepared from a mixture of TFA-pretreated Aβ in TFE and PC lipids in methanol/chloroform (see Materials and Methods). When the solvents were slowly removed with a nitrogen flow, due to its higher vapor pressure, chloroform rapidly evaporated and the peptide-lipid mixed film was thus essentially deposited from a TFE-methanol mixture (~2:1 volume ratio). The CD spectrum of TFA-pretreated Aβ redissolved in TFE/methanol (2:1, v/v) is given in Figure 1; the cross-over point at 201 nm and the two minima near 208 and 222 nm show that the Aβ peptide is almost entirely helical in this solvent mixture.[56] No precipitation was observed during solvent removal and the dried film had a homogeneous smooth appearance, indicating that demixing of peptide and lipid did not occur upon drying.

Characterization of mixed film-derived proteoliposomes

Hydration of the dry mixed film of Aβ and POPC with buffer solution resulted in the formation of a vesicle suspension, which was investigated with wide-line ^{31}P NMR spectroscopy to assess the vesicle morphology. The configuration and dynamics of the phosphorus-containing lipid head groups are reflected in the shape of the ^{31}P NMR spectrum, and because the rotation of large vesicles is slow on the ^{31}P NMR time scale, the spectral width relates to the vesicle size. The ^{31}P NMR spectrum of a peptide-free POPC vesicle dispersion (Figure 2(a)) is characterized by a low-field shoulder near 30 ppm and a high-field peak at −16 ppm, typical for multilamellar vesicles of phospholipids in the liquid-crystalline phase.[57,58] The spectrum of a dispersion of Aβ/POPC vesicles (Figure 2(b)) is essentially identical, with the same spectral width, or residual chemical shift anisotropy (CSA), of approximately -46 ppm, indicating that the presence of 2 mol% Aβ in the dry lipid film was compatible with vesicle formation. The spectra in Figure 2(a) and (b) also contain a minor isotropic signal at −1.5 ppm, representing a small amount of unilamellar vesicles that tumble rapidly on the ^{31}P NMR time scale.[57,58]

For pure-lipid and Aβ/lipid mixed film samples, the average order of the perdeuterated acyl chain of POPC-d_{31}, which is related to the quadrupolar splitting from each deuterated chain segment,[59,60] was investigated by wide-line ^{2}H NMR spectroscopy. ^{2}H NMR spectra of multilamellar vesicles in the absence and presence of Aβ were identical, with quadrupolar splittings ranging from 2.6 to ~25.5 kHz (spectra not shown), typical for unperturbed fluid-state acyl chains.[61] Also in ^{31}P and ^{2}H NMR studies in which unstructured Aβ40 or Aβ42 had associated to multilamellar vesicles consisting

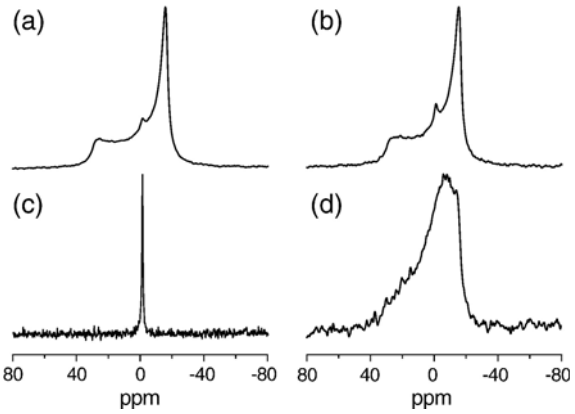

Figure 2. ^{31}P NMR spectra of dispersions of (a) pure POPC and (b) Aβ/POPC vesicles, and of the (c) supernatant and (d) pellet fraction of a sonicated and centrifuged Aβ/POPC dispersion. The spectra are recorded in excess water at 23 °C.

of POPC and negatively charged POPG or POPS lipids through electrostatic interactions (after hydration of a dried lipid film with Aβ-containing buffer solution), no significant effect on multilamellar vesicle morphology is evident.[29,62]

The Aβ/PC proteoliposome dispersion was extruded or sonicated to convert the multilamellar vesicles to small unilamellar vesicles, which are suitable for CD and other optical spectroscopies. Sonicated suspensions were centrifuged to separate the unilamellar vesicles from any remaining larger structures, and ^{31}P NMR spectra of the pellet and supernatant fractions were recorded. The spectrum of the supernatant fraction (Figure 2(c)) consists only of an isotropic resonance at −1.4 ppm, as expected for unilamellar vesicles. The ^{31}P NMR spectrum of the pellet fraction (Figure 2(d)) is similar to that of the unsonicated multilamellar vesicle dispersion, although next to the main wide-line spectral component with a CSA of approximately −46 ppm, there are also components with a smaller CSA present, indicative of multilamellar vesicles of a reduced size. ^{2}H NMR spectra of the supernatant and pellet fraction were also characterized by isotropic and multi-component wide-line resonances, respectively (data not shown). Since in the absence of Aβ, PC liposomes can be readily transformed in unilamellar vesicles by sonication, the Aβ peptide apparently renders the multilamellar vesicles less susceptible to such morphology changes. It can thus be envisaged that the vesicles with a higher Aβ content are present in the pellet fraction and that the unilamellar vesicles, which are present in the supernatant fraction, have a somewhat reduced Aβ content.

CD spectra of different unilamellar proteoliposomes are shown in Figure 3. The spectra of Aβ associated with fluid-state POPC and gel-state DPPC vesicles are almost identical. The cross-over point at 209 nm and a single minimum around 219 nm, correspond to an Aβ40 peptide that is entirely β-structured. The spectrum of Aβ40 in mixed vesicles of POPC and POPE is slightly shifted to lower wavelengths, whereas the addition of ergosterol (for vesicle fusion experiments; see below) leads to a more pronounced shift. The latter spectrum has a cross-over point of 207 nm and a minimum near 218 nm, indicating the presence of 10–20% helical or random coil structure. For comparison, the conformation of commercially obtained Aβ42 was also investigated. The CD spectrum of TFA-pretreated Aβ42 re-dissolved in TFE/methanol (2:1, v/v) was characterized by a cross-over point at 201 nm and two minima near 208 and 222 nm, and the spectrum of Aβ42 with POPC vesicles by a cross-over point of 207 nm and a single minimum near 218 nm (data not shown). Thus the longer and more hydrophobic Aβ42 is also almost entirely helical in the solvent mixture from which the mixed film is prepared, but predominantly β-structured in the proteoliposomes that are obtained by hydration of this film.

Channel-like activity of Aβ in uncharged bilayers

The effect of the β-structured Aβ40 peptide on the structural integrity of uncharged phospholipid bilayers was investigated with electrical measurements. To this end, a planar bilayer suspended over a 150 μm diameter connection between two aqueous compartments was voltage clamped, and the bilayer current was recorded before and after fusion of Aβ-containing vesicles into the bilayer (see Materials and Methods). The planar bilayer and the vesicles consisted of POPC as well as the fusion-enabling zwitterionic lipid POPE. This composition facilitates the interpretation of bilayer currents because soluble (monomeric) Aβ is unable to increase the conductivity of zwitterionic planar bilayers.[40,81] The vesicles also contained composite ion channels of the polyene antibiotic nystatin and the sterol ergosterol. These channels render the vesicles more fusogenic and have the additional advantage that their introduction into the planar bilayer results in a

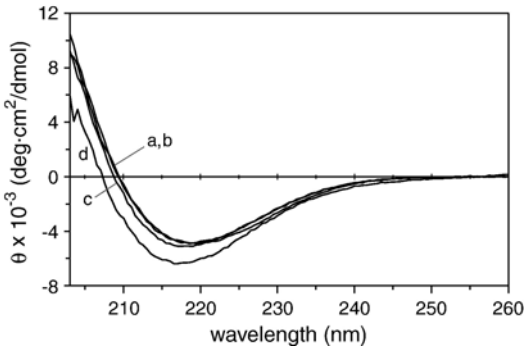

Figure 3. Circular dichroism spectra of unilamellar vesicles of (a) Aβ/POPC, (b) Aβ/DPPC, (c) Aβ/POPC-POPE (2:1 lipid molar ratio), and (d) Aβ/POPC-POPE-ergosterol (6:3:1 molar ratio). Spectra are recorded at ambient temperature and are corrected for the spectral contribution of the lipids.

readily detectable bilayer current that clearly marks each individual vesicle fusion event.[63,64]

Unilamellar mixed film-derived proteoliposomes (Aβ40/total lipid = 1:200, molar ratio) with nystatin-ergosterol channels were added to the *cis* side of a planar bilayer, and the bilayer current was monitored at the applied potential of +100 mV. As can be seen in the current trace depicted in Figure 4(a), the current is initially at noise level (<1 pA), illustrating the negligible conductance of an unperturbed lipid bilayer. About 45 s after vesicle injection, the current suddenly jumps to 19 pA, corresponding to a bilayer conductance of 190 pS, and then gradually decays for ~15 s until the next current jump. The sudden increase in bilayer current is caused by the incorporation in the planar bilayer of open nystatin-ergosterol channels, and marks a single vesicle fusion event. The subsequent gradual current decay is the result of the gradual dissociation of these composite channels, which are unstable in the ergosterol-free planar bilayer.[63,64] The current trace in Figure 4(a) shows three vesicle fusion events, at approximately 45, 60 and 74 s after vesicle injection. Whereas the current decay that follows the first vesicle fusion event is characterized only by the disintegrating nystatin-ergosterol channels, the electrical "activity" superimposed on the current decay of the second vesicle is caused by vesicle-associated Aβ. This activity becomes more frequent after fusion of the third vesicle, indicating that this vesicle has delivered additional Aβ to the planar bilayer.

The activity of Aβ itself can be studied when the nystatin-ergosterol channels have completely dissociated, which typically takes several minutes. Expanded views of the current trace near 88 s are depicted in Figure 4(b) and (c). There is some residual nystatin-ergosterol current at this point in the current trace, but the Aβ activity can clearly be

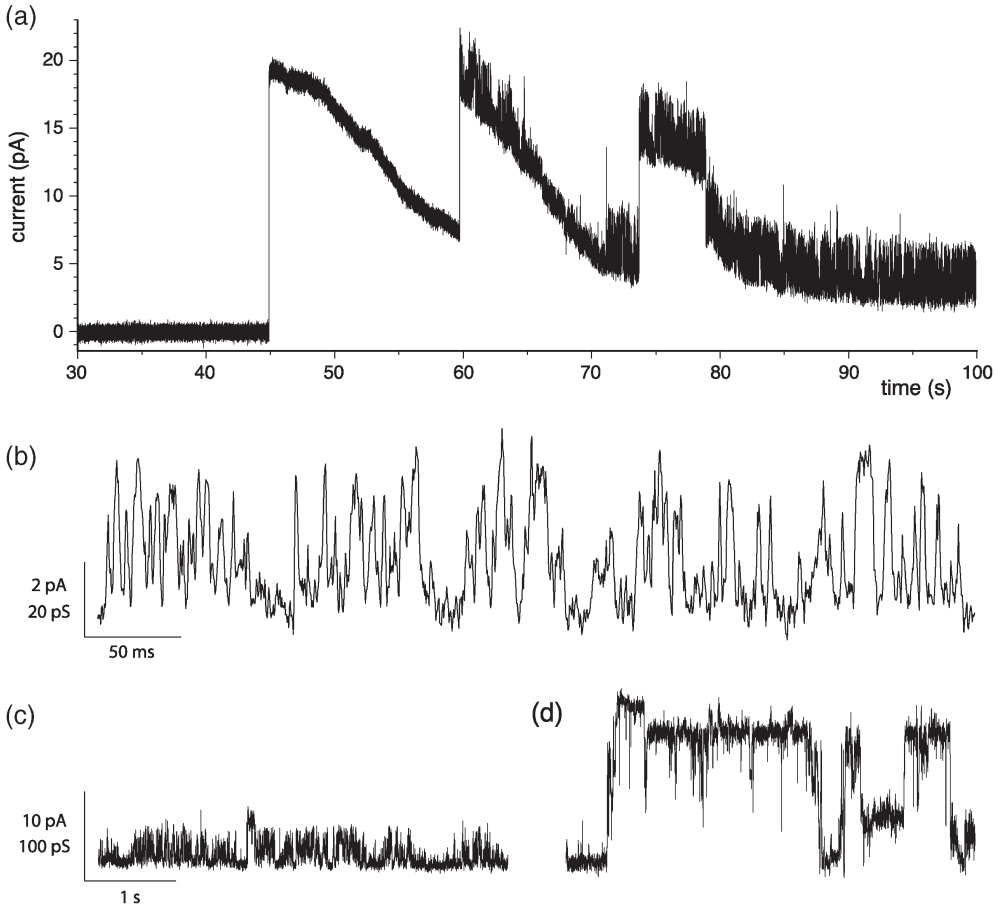

Figure 4. Current traces of a planar bilayer of POPC/POPE (3:7 molar ratio) voltage clamped at +100 mV, recorded after addition to the *cis* side of the planar bilayer of vesicles of POPC-POPE-ergosterol (6:3:1 molar ratio) that contain Aβ and the polyene antibiotic nystatin. (a) The abrupt current increase at ~45, 60 and 74 s after vesicle addition corresponds to the subsequent fusion of three individual vesicles with the planar bilayer. Vesicle fusion introduces composite nystatin-ergosterol channels in the planar bilayer, but because these channels gradually dissociate in the ergosterol-free planar bilayer, their contribution to the bilayer current decreases immediately after vesicle fusion.[63,64] The vesicles also deliver Aβ peptides to the planar bilayer; intermittent Aβ-induced current spikes are apparent after fusion of the second vesicle and Aβ electrical "activity" becomes continuous after more Aβ has been delivered by the third vesicle. (b) Expanded view of the current trace at 88 s after vesicle addition. The constant value of the residual nystatin-ergosterol current enables observation of the Aβ-induced bilayer current. (c) Expanded view (87.5–92.0 s) of the current trace after three vesicle fusion events, and (d) approximately 2 min later, after fusion of five more vesicles (not shown in (a)). The traces depicted in (c) and (d) are at the same scale; an increased amount of Aβ in the planar bilayer has resulted in increased Aβ activity.

distinguished from the stable nystatin-ergosterol current baseline of ~2 pA. The Aβ-induced current is characterized by short (<10 ms) spikes, which occur with high frequency (~100–200 Hz) and have a variable conductance of up to 50 pS (Figure 4(b)). This is similar to the "spiky fast cation channel" mode as described for soluble Aβ after electrostatic association with planar bilayers consisting of POPE, POPC and the negatively charged lipid POPS.[41,42] Significantly higher conductances have also been reported under the same experimental conditions, and it has been hypothesized that this heterogeneity reflects different channel conformations of Aβ rather than the association of more peptide material with the bilayer.[41,42] However, when the recording of Figure 4(a) was continued and several vesicles had delivered additional Aβ to the planar bilayer, the Aβ activity, characterized by conductances of up to ~200 pS and an increased open channel lifetime (see Figure 4(d)), resembled the distinctly different "medium conductance" mode of Aβ in negatively charged planar bilayers.[41]

Aβ disruption of supported PC bilayers

The topography of supported bilayers formed by the spontaneous rupture of unilamellar vesicles on a mica substrate was investigated in aqueous solution by atomic force microscopy (AFM). As can be seen in Figure 5(a), a bilayer of pure POPC is flat, with a surface roughness of 0.2 nm or less, except for the presence of unfused vesicles that are adsorbed to the bilayer surface. As expected for a supported bilayer of pure POPC, the distance from the mica to the bilayer surface, as measured at the edges of a bilayer patch or at a bilayer defect, was ~4.2 nm (data not shown). A supported bilayer formed from Aβ40/POPC vesicles (Figure 5(b) and (c)) was initially also characterized by a surface roughness of ~0.2 nm (at sufficient distance from the bilayer edge) and a bilayer thickness of approximately 4.5 nm, as revealed in the height profile (Figure 5(d)) corresponding to the cross-section of the Aβ/POPC island shown in Figure 5(c). There was no sign (either in the height, phase, or amplitude images) of Aβ assemblies, but small (<10 nm lateral dimension) topological features are difficult to detect in fluid bilayers like POPC.

The two bilayers were further investigated with force spectroscopy measurements, in which the deflection of the cantilever is indicative of the forces experienced by the cantilever tip.[65] When a negatively charged cantilever tip was gradually moved toward the bilayer, the cantilever deflection remained constant until the tip came in close proximity to the bilayer surface (Figure 5(e)). At this point, for the pure POPC bilayer, the cantilever was subject to a negative deflection, indicating that

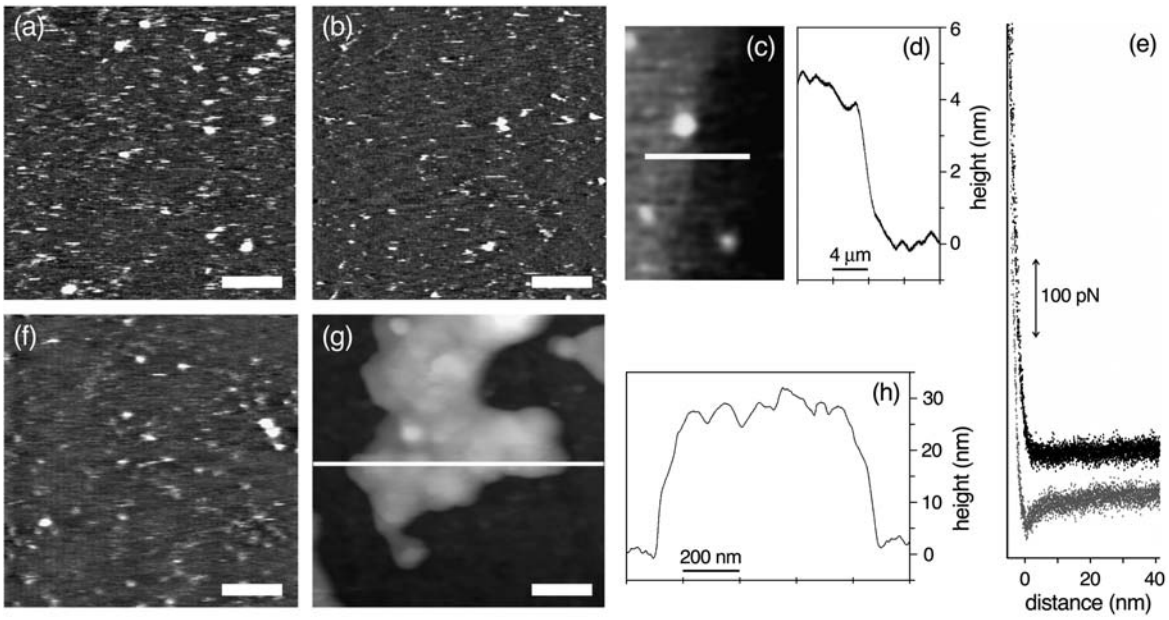

Figure 5. AFM analysis of supported bilayers in aqueous solution. Topography image with 1.0 nm *z*-range of supported bilayers of (a) pure POPC and ((b) and (c)) Aβ/POPC formed by rupture of unilamellar vesicles on mica: the bilayer surface is grey with lighter and darker grey features (indicating a surface roughness of <0.2 nm), unfused vesicles on top of the bilayer are white and uncovered mica is black. (d) The height profile of the Aβ/POPC island edge as indicated in (c) shows that the thickness of the Aβ/POPC bilayer is ~4.5 nm. (e) Force-distance curves for the approach of a negatively charged cantilever tip toward the bilayers depicted in (a) and (b): the tip–sample interaction is dominated by Van der Waals attraction close to the POPC surface (grey curve) but not close to the Aβ/POPC surface (black curve). (f) Topography image of the pure POPC bilayer, incubated for two weeks at +4 °C: the bilayer surface is represented by grey shades and unfused vesicles on top of the bilayer are white (1.0 nm *z*-range). (g) Topography image of the Aβ/POPC bilayer, incubated for two weeks at +4 °C: exposed mica is black, amorphous material is grey to white (30 nm *z*-range). (h) Height profile of the cross-section indicated in (g). The images (a), (b), (f) and (g) are 1.0 μm × 1.0 μm, 256 × 256 pixels, with 200 nm scale bar, and (c) is 25 μm × 40 μm, with 16 μm cross-section.

attractive (Van der Waals) forces dominate the tip–sample interaction.[65,66] When moved even further toward the bilayer surface, the tip cannot physically proceed without penetrating the bilayer and, therefore, the force experienced by the cantilever tip becomes rapidly repulsive (Figure 5(e)). However, in close proximity to the surface of the Aβ/POPC bilayer, there is no attractive regime, indicating that the negatively charged tip experiences an electrostatic repulsion that dominates the tip–sample interaction.[65] Since the Aβ peptide is overall negatively charged at pH 7.4, this confirms the presence of Aβ.

As in previous studies where soluble Aβ was added to preformed supported bilayers,[38,67] the samples were imaged again after an incubation period during which the bilayers were kept hydrated in buffer solution. The topography of the pure POPC bilayer (Figure 5(f)) had not changed after two weeks at 4 °C but, as can be seen in Figure 5(g), the appearance of the Aβ/POPC sample had changed dramatically. Rather than a smooth bilayer of 4 nm thickness with no distinguishing surface features, the Aβ/POPC sample now consisted of amorphous structures with a height of up to 50 nm, separated by areas of exposed mica. A typical height profile of these structures, protruding ~30 nm from the mica, is shown in Figure 5(h). This material was only weakly associated with the mica substrate and could easily be displaced by the AFM tip. The initially well-defined Aβ40/POPC bilayer had thus completely disintegrated during the incubation period. However, no fibrillar amyloid could be observed and the amorphous structures appeared homogeneous in height, phase and amplitude in AFM images (data not shown), suggesting that they had formed a relatively uniform Aβ40-lipid aggregate. A similar morphology has also been observed after exposure of supported DMPC bilayers to an Aβ42-containing aqueous solution.[38]

Conformation of Aβ in supported PC multilayers

Supported Aβ40/PC multilayers were formed on top of a germanium crystal by removing excess water from a dispersion of multilamellar or sonicated unilamellar vesicles that were prepared by the mixed film method. Attenuated total reflection Fourier transform infrared (ATR-FTIR) spectra were recorded to characterize the conformation of Aβ in these supported planar bilayers. The expanded spectrum of pure POPC multilayers (Figure 6(a), curve a) shows a signal around 1736 cm^{-1} that corresponds to the lipid ester stretch vibration.[68] This peak was used to normalize the spectral intensity. FTIR spectra of supported bilayers formed from unilamellar and multilamellar Aβ/POPC proteoliposomes are also depicted in Figure 6(a) (curve b and c, respectively). The additional component between ~1700 and 1600 cm^{-1} in these spectra, the amide I band, is the most intense polypeptide absorption band.[68] The relative spectral intensities of the lipid C=O and amide I bands are typical for the employed peptide/lipid molar ratio of 1:50, and the amide I contribution was approximately twice as intense for control samples with a peptide/lipid molar ratio of 1:25 (data not shown).

The amide I band arises mainly from the carbonyl vibration ν(C=O) contribution from the amide bond and can, therefore, be used to characterize peptide backbone conformation. The spectra of Aβ/POPC multilayers prepared from unilamellar and multilamellar vesicles displayed a prominent feature at 1626 cm^{-1}, characteristic for peptides in a β-sheet conformation. The observed weak signal at ~1695 cm^{-1} has been used to refine this assignment to antiparallel β-sheets,[69] but since it has also been observed for amyloid fibrils which, according to solid-state NMR structure determination,[16,17] are composed of parallel β-sheets,[70] this distinction may not be meaningful. A detailed analysis of the secondary structure of Aβ in different lipids was performed by curve-fitting of the amide I band (see Materials and Methods), the result of which is shown in Figure 6(b) for Aβ/POPC multilayers prepared from unilamellar vesicles. The analysis of the amide I band is consistent with the presence of

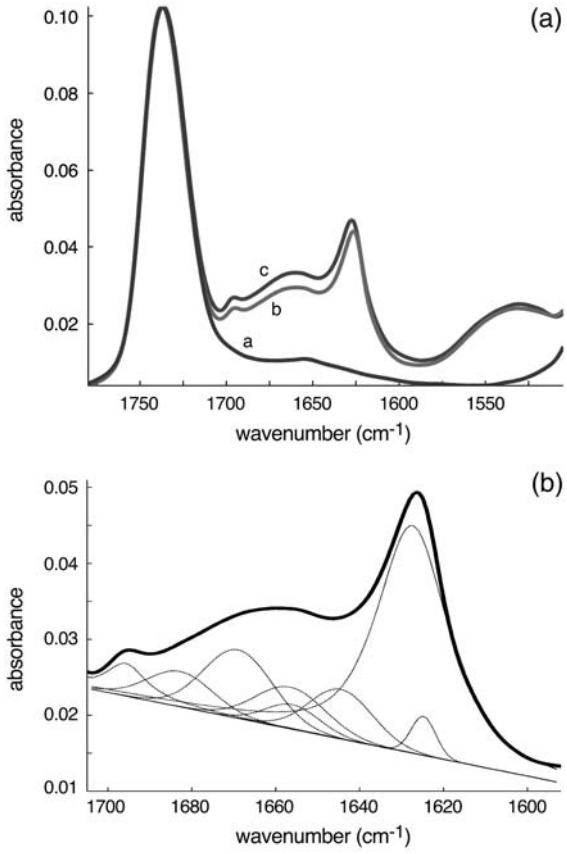

Figure 6. Baseline-corrected and atmospheric water-subtracted ATR-FTIR spectra, normalized on the lipid carbonyl band at ~1740 cm^{-1}. (a) Lipid carbonyl band of multilayers of pure POPC (curve a) and lipid carbonyl and amide I band of multilayers formed from Aβ/POPC SUVs (curve b) and Aβ/POPC MLVs (curve c). (b) Curve-fitting analysis of the amide I band of multilayers formed from Aβ/POPC SUVs.

66% β-sheet, 22% α-helix, 6% turn and 6% random coil structure. Analysis of Aβ/POPC multilayers deposited from a multilamellar vesicle suspension yielded similar values: 70% β-sheet, 14% α-helix, 15% turn and 2% random coil. These values did not change significantly over a period of two weeks (data not shown).

Discussion

Bilayers of zwitterionic lipids, particularly phosphatidylcholine species, present the most simple model membrane system but their interaction with Aβ peptides is poorly understood because soluble monomeric Aβ does not undergo a conformational change in the absence of acidic lipids or glycolipids. Here we investigated the conformation and organization of Aβ40 in zwitterionic model membranes and assessed its effect on bilayer integrity. We used the mixed film method in an attempt to ensure association of Aβ40 with net uncharged bilayers, and observed effects on both the Aβ peptides and the bilayers that are remarkably similar to those reported for Aβ association from the aqueous phase with more complex membranes. These results and their implication for the mechanism of Aβ-induced membrane perturbation are discussed here.

Conformation of membrane-associated Aβ

Because with optical spectroscopies the Aβ signal is difficult to separate from the background absorbance of natural membranes and total lipid extracts, the secondary structure of membrane-associated Aβ has almost exclusively been studied with model membrane systems. Terzi *et al.* demonstrated with CD that the conformation of Aβ40 changes from predominantly random coil to about equal percentages of random coil and β-structure upon exposure to preformed acidic vesicles of POPC/POPG (3:1 molar ratio) at a peptide/lipid molar ratio of 1:50, but raising the salt concentration to a more physiological value of 100 mM NaCl abolished the formation of secondary structure, even for vesicles of pure POPG.[12] Recent infrared reflection and grazing incidence X-ray diffraction studies,[35–37] in which only the Aβ peptides in close proximity to compressed monolayers are detected, indicated that initially unstructured Aβ40 assembles as β-sheets which are oriented parallel to the surface of anionic (and also cationic) monolayers, but only in the absence of salt when electrostatic interactions can drive membrane association.[12,29,32,33] McLaurin & Chakrabartty showed with CD that at physiological ionic strength and pH 7.0, Aβ42 but not Aβ40 adopts β-structure in the presence of acidic vesicles, whereas at pH 6.0 both Aβ species adopt β-structure.[27,28] However, a helical content of up to ~40% was also observed after association with POPG-containing vesicles, although only in the absence of salt ions.[29,71] In none of the above studies was soluble primarily unstructured (i.e. monomeric) Aβ40 or Aβ42 shown to undergo a conformational change in the presence of zwitterionic vesicles or monolayers of PC or PE.

Acidic phospholipids are not the only components that can induce folding of Aβ peptides. Zwitterionic model membranes containing the glycolipid ganglioside G_{M1} cause a structural transition, at physiological ionic strength, to either primarily β-structure, primarily α-helix or a mixed α/β structure, depending on the pH value and the Aβ/ganglioside ratio.[24,27,71,72] This is facilitated in the presence of cholesterol, and potentially by lipid rafts in general.[72] Although the presence of the divalent metal ions Cu^{2+} and Zn^{2+} has also been reported to result in a primarily helical conformation of Aβ42 in the presence of acidic POPC/POPS vesicles at a high Aβ/lipid ratio of 1:7,[30] it should be noted that these ions cause folding of Aβ40 in the absence of vesicles as well.[73] Model membrane studies in which primarily unstructured Aβ is added to suspensions of preformed vesicles thus do not point to a single membrane-induced conformational motif for Aβ, and indicate that at physiological ionic strength and pH 7.4, monomeric Aβ can only associate with membranes under specific conditions.

The mixed film method for Aβ association with model membranes has only sporadically been employed in conformational studies. ATR-FTIR spectra of Aβ40 in multilayers of egg yolk PC and ganglioside G_{M1} (1:50 Aβ/lipid molar ratio), obtained from hydration with salt-free ^2H_2O of a mixed film dried from HFP, were consistent with a β-sheet content of 80%, with the plane of the β-sheets oriented parallel to the bilayer surface.[71] Bokvist *et al.* prepared peptide-lipid films from a mixture of Aβ40 in TFA and DMPC-DMPG in chloroform/methanol (3:1, v/v) with an Aβ/lipid ratio of 1:30.[33] CD spectra of the corresponding unilamellar vesicles at physiological ionic strength and pH 7.8 and in the presence of EDTA (to prevent interaction with divalent metal ions) showed that for pure DMPC vesicles, Aβ40 was present as a ~60:40 mixture of β-structure and random coil, whereas for pure DMPG vesicles, the conformation of Aβ40 consisted of about equal amounts of β-structure, α-helix, and random coil.[33] For the most complex mixed film samples studied to date, PC, PS, PE, sphingomyelin, cholesterol, cerebroside and ganglioside G_{M1} (mimicking the composition of cerebral cortex membranes) in chloroform were mixed with Aβ40 in HFP at a Aβ/lipid molar ratio of 1:20, and unilamellar vesicles prepared from the mixed film were investigated with CD.[74] At physiological ionic strength and pH 7.4, Aβ40 was found to be initially unstructured, indicating expulsion from the lipid bilayer, but the peptide had adopted 60% β-structure after one day of incubation. In the absence of ganglioside and cholesterol, secondary structure was immediately apparent for Aβ40, with the percentage of β-structure increasing over a period of several days.[74]

Aβ40 and Aβ42 are helical in the solvent mixture that was used in the present study to obtain mixed

films of Aβ and POPC with a 1:50 molar ratio, but are shown by CD to be primarily β-structured in unilamellar vesicles (Figures 1 and 3). Additionally, ATR-FTIR measurements demonstrate that Aβ40 is primarily present as β-sheets in supported multilayers obtained by fusion of unilamellar and multilamellar proteoliposomes (Figure 6). Given the significant percentage of helical structure of Aβ40 in methanol and HFP (see Figure 1) and the rapid evaporation of chloroform, it can be assumed that Aβ40 was also helical in the dried mixed films of the studies cited above. Yet, with an apparent exception for bilayers with a high acidic lipid content,[33] the different lipid compositions all result in Aβ40 that is primarily β-structured.[33,71,74] Since hydrophobic peptides, provided that their hydrophobic segment is of sufficient length, can generally be incorporated as transmembrane α-helices with the mixed film method,[49,50] it is significant that this topology is not observed in lipid mixtures ranging from complex neuronal membrane mixtures[74] to simple fluid bilayers of POPC, which are relatively thin. Therefore, it is highly unlikely that *in vivo* Aβ40 or Aβ42 is able to retain a helical transmembrane topology after proteolytic processing of amyloid precursor proteins,[8] or that helical bundles of Aβ peptides can insert into the membrane to form ion channels.[51]

Oligomerization state of membrane-associated Aβ

Only the highest-order assembly state of Aβ peptides, the mature amyloid fibril, has been characterized in atomic detail; solid-state NMR and X-ray diffraction data are consistent with an unstructured N terminus and a C-terminal β-strand–turn–β-strand fold of individual peptides, which are stacked as intermolecular in-register parallel β-sheets with backbone hydrogen bonding in the direction of the fibril axis.[16,17] However, a multitude of lower-order oligomerization states, collectively referred to as "soluble oligomers", have been identified *in vitro* by AFM and electron microscopy. The morphology of these is usually spherical, with diameters ranging from about 2 to 30 nm.[13,14,18,75,76] Structural information about soluble oligomers is scarce, particularly for the larger particles, although these could possess β-structure.[18,19] Circular dichroism studies of low-*n* oligomers (up to hexamers) of Aβ, identified by analytical ultracentrifugation or gel electrophoresis and isolated by size-exclusion chromatography, have reported irregularly structured,[19] primarily unstructured,[77] and also primarily β-structured[78] conformations. It has also become clear from this work that low-*n* oligomers are rapidly formed *in vitro* unless oligomerization seeds are removed by pretreatment of synthetic Aβ with either HFP[14] or TFA.[79]

Only a limited number of studies have addressed the morphology of model membrane-associated Aβ. McLaurin and co-workers added TFA-pretreated unstructured Aβ to preformed supported bilayers and monitored the evolution of the bilayer topography with AFM at physiological ionic strength and pH 7.4.[38,67] Bilayers of total brain lipid extract (containing acidic lipids, gangliosides and cholesterol) exposed to an aqueous solution of Aβ40 initially showed scattered protrusions with a height of ~1 nm and a diameter of 1–2 nm, suggested to represent partially inserted Aβ40 monomers. This was followed by fibril growth through the bilayer with concomitant excison of large bilayer patches.[38] Also gel-state bilayers of DMPC initially showed small protrusions when exposed to a solution of Aβ40, but in time these developed to globular aggregates (up to 10 nm in size) while the bilayer remained largely intact.[38] Significantly, addition of preformed Aβ40 fibrils and globular aggregates to supported bilayers led only to their deposition on the bilayer surface, not to bilayer disruption, indicating that lipid-modulated oligomerization of Aβ40 is required for membrane destabilization.[38]

As described above, the mixed film method has been used to associate Aβ40 with model membranes mimicking neuronal membranes.[74] EM analysis of initially multilamellar vesicle dispersions showed extensive fibril formation around aggregated vesicles. But in the absence of cholesterol and ganglioside G_{M1}, only a size reduction of the vesicles was observed. This "solubilization" of the multilamellar vesicles, which still contained a variety of (acidic) lipid components, was attributed to membrane-associated Aβ40.[74] Lin *et al.* used unilamellar vesicles, obtained by hydration of a mixed film of Aβ42 and DOPC that was deposited from 100% chloroform, to prepare a supported bilayer for AFM characterization.[43] Ring-shaped structures with an outer diameter of 8–12 nm were found to protrude ~1 nm from the surface of the fluid DOPC bilayer, and were interpreted as the extramembranous part of a ring of between four and six transmembrane Aβ peptides that line an ion channel pore.[43] However, the combined observations that ring-like Aβ42 oligomers can be formed in the absence of lipid[75] and the insolubility of Aβ40 in chloroform (Figure 1), render it unlikely that these ring-shaped topography features traverse the bilayer (and thus represent a transmembrane channel configuration of Aβ). The similar ring-like features that were observed on a supported fluid bilayer formed from a dispersion of unilamellar DOPC vesicles to which untreated, potentially oligomerized, Aβ was added,[45] are also unlikely to represent a transmembrane configuration of Aβ peptides.

In the present study, the unilamellar vesicles that were used to form a supported Aβ40/POPC bilayer are prepared from an organic solvent mixture in which the lipid, as well as the peptide, components are soluble, thus preventing peptide-lipid segregation in the dry film. The supported bilayer initially appears structurally sound, with no sign of bilayer defects or topological features that can be attributed to Aβ (Figure 5(b)). AFM force measurements indicate an electrostatic repulsion of a negatively charged cantilever tip, which does not occur for pure

POPC bilayers, thus confirming the presence of Aβ40 in the POPC bilayer. Since Aβ40 assemblies are not resolved by AFM, and CD and ATR-FTIR measurements indicate that its conformation is primarily β-sheet in vesicles and supported multilayers of POPC, it can be assumed that Aβ40 is present as structured or "collapsed" monomers[78] or as small low-*n* oligomers, intimately associated with the fluid POPC bilayer. The Aβ peptides may either be completely or partially buried in the bilayer; the detection of small topological features of sterol-free fluid bilayers by AFM is not trivial. The influence of Aβ40 became manifest after prolonged incubation; the supported bilayer disintegrated into amorphous aggregates, most likely composed of both lipids and peptides, that are up to 50 nm high (Figure 5(g)). These resemble the smaller aggregates that are observed after prolonged exposure of a supported DMPC bilayer to soluble Aβ40.[38] The formation of these aggregates on a solid support could be a different manifestation of the Aβ–lipid interactions that cause the breakdown of (cholesterol and ganglioside-free) brain lipid vesicles into smaller vesicles with a higher curvature.[74]

Mechanism of membrane perturbation

Disregarding an interaction of Aβ with endogenous calcium channels,[47] which cannot be investigated with protein-free model membranes, Aβ-induced disruption of calcium homeostasis originates either from the formation of transmembrane ion channels of Aβ multimers[80] or from a non-specific perturbation of bilayer integrity.[46] Electrical bilayer recordings of acidic bilayers or sterol-containing zwitterionic bilayers demonstrate that Aβ40 and Aβ42 can associate from the aqueous phase and modulate the conductance of suspended planar bilayers in a manner that has been described as channel-like.[39,40,42,81] Ion channels typically have only a single or a limited number of well-defined conductance states, but Aβ gives rise to a very wide range of conductances (4–4000 pS), with high-frequency "spiky" conductance variations and frequent abrupt transitions to the closed state, also from the highest conductance levels.[41,81,82] The flickering between (extreme) conductance states has been attributed to changes in the molecular organization of a single channel rather than the addition or elimination of Aβ peptides.[41,42] In these experiments, the Aβ peptides have not been pretreated to remove aggregation seeds and Aβ is therefore likely to have been present in a variety of oligomerization states. In a recent study, spherical oligomers of Aβ42 (3–5 nm diameter with an apparent molecular weight of ~100 kDa) were shown to increase the conductance of planar bilayers to ~8000 pS, without any evidence of discrete channel behavior or ion selectivity, whereas exposure to monomers/dimers or fibrils of Aβ42 had no effect.[46]

Introduction of Aβ40 into a zwitterionic planar bilayer by fusion of Aβ40-containing vesicles, prepared with the mixed film method, gave rise to the channel-like electrical activity that is typically observed for soluble Aβ (Figure 4). Each vesicle fusion event was clearly marked by the introduction of transient nystatin-ergosterol channels, which makes it possible to correlate the electrical activity with the amount of Aβ delivered to the planar bilayer. Continued vesicle fusion resulted in a gradual increase in the maximum conductance, from ~50 to 200 pS (Figure 4), indicating that the different modes of channel-like activity[41] are related to the amount of bilayer-associated Aβ and not to conformational flexibility of a single transmembrane Aβ channel. It should also be noted that each vesicle should contain several orders of magnitude more Aβ than required for the formation of a single channel. Assuming that the conformation of vesicle-associated Aβ40 does not change upon vesicle fusion with the planar bilayer, which is unlikely since the peptide adopts predominantly β-structure in both unilamellar vesicles and multilayers formed by fusion with other vesicles (Figures 3 and 6), it can be concluded that the typical channel-like behavior of Aβ is not caused by helical bundles of transmembrane Aβ peptides. Moreover, the lack of distinct topographical features in supported bilayers derived from fusion of Aβ40/POPC vesicles (Figure 5(b)) argues strongly against the assembly of Aβ peptides into any type of discrete ion channel.

For the Aβ40/POPC model system, the combined observations instead argue for a non-specific perturbation of bilayer integrity by small Aβ assemblies, with a large proportion of β-sheet structure, which are embedded in the lipid bilayer. If this conformation is similar to the organization of Aβ in mature fibrils, the hydrophilic N terminus of the peptides will be unstructured while the longer C-terminal hydrophobic part will be present in a β-strand–turn–β-strand fold. In this configuration, the N terminus, if not protruding from the bilayer, would only be able to associate with the polar lipid head group region. However, the C-terminal hydrophobic side-chains and the (partial) inter-strand hydrogen bonding between amide bonds could allow a deeper bilayer localization of this segment, potentially near the polar–apolar interface of the bilayer, slightly below the lipid glycerol backbone. Such a partial penetration of the lipid bilayer, commonly observed for membrane-targeting toxins such as the amphipathic peptide melittin, is sufficient to induce transient lipid packing defects with concomitant loss of bilayer integrity.[83]

Soluble Aβ assemblies, potentially in particular low-*n* oligomers of Aβ42, have recently been identified as the primary pathogenic Aβ species *in vivo*,[4,5,52,53] and constitute the most potent bilayer perturbers *in vitro*.[46–48] Since soluble oligomers of Aβ permeabilize model membranes and neuroblastoma cells, and soluble oligomers of peptides from other protein misfolding diseases have a similar effect,[46,47,84] it seems likely that the amphipathic nature of Aβ and its oligomers is necessary but also

sufficient for membrane association and subsequent destabilization.

With the mixed film method, low-*n* oligomers of Aβ40 could have formed after initial expulsion of Aβ40 from the POPC bilayer. The bilayer perturbation observed for Aβ40/POPC is expected to be more pronounced for Aβ42 because this analog oligomerizes more readily than Aβ40,[14] and also for more complex membranes because these facilitate association of (monomeric) Aβ. Oligomer–membrane interactions could be further investigated by exposing bilayers of various lipid compositions to a series of well-defined *n*-oligomers of Aβ40 and Aβ42, with subsequent characterization of the bilayer permeability and topography and the peptide conformation and orientation with respect to the membrane.

Materials and Methods

All phospholipids were purchased from Avanti Polar Lipids (Alabaster, AL). TFA, TFE, chloroform and decane were obtained from Aldrich (St. Louis, MO), and methanol, ethanol, HFP, heptane and hexane were supplied by Fisher Scientific (Loughborough, UK). All solvents were >99% pure, except ethanol (95%). Aβ42, nystatin dihydrate and ergosterol were obtained from Sigma (St. Louis, MO).

Peptide synthesis and purification

The peptide sequence, H-Asp(OtBu)-Ala-Glu(OtBu)-Phe-Arg(Pbf)-His(Trt)-Asp(OtBu)-Ser(tBu)-Gly-Tyr(tBu)-Glu(OtBu)-Val-His(Trt)-His(Trt)-Gln(Trt)-Lys(Boc)-Leu-Val-Phe-Phe-Ala-Glu(OtBu)-Asp(OtBu)-Val-Gly-Ser(tBu)-Asn(Trt)-Lys(Boc)-Gly-Ala-Ile-Ile-Gly-Leu-Met-Val-Gly-Gly-Val-Val-O-Wang-Argogel (abbreviations of protecting groups: Trt, trityl; Pbf, 2,2,4,6,7-pentamethyldihydrobenzofuran-5-sulfonyl; tBu, tert-butyl; Boc, tert-butyloxycarbonyl), representing the amino acid sequence of human β-amyloid(1-40), was synthesized automatically on an Applied Biosystems 433A Peptide Synthesizer using the FastMoc protocol[85] on 0.25 mmol scale. N^{α}-9 fluorenylmethoxycarbonyl (Fmoc)-Val-OH was coupled to the Wang resin[86] using the method described by Sieber[87] and this was used to obtain the C-terminal peptide acid. Coupling of N^{α}-Fmoc amino acids (1 mmol, four equivalents) was performed with 2-(1H-benzotriazol-1-yl)-1,1,3,3-tetramethyluronium hexafluorophosphate/*N*-hydroxybenzotriazole (HBTU/HOBt) in the presence of eight equivalents of *N*,*N*-diisopropylethylamine (DIPEA) in *N*-methylpyrrolidone (NMP) for 45 min. The coupling of the first three C-terminal amino acid residues (Gly-Gly-Val) was carried out with HBTU/HOBt/DIPEA in NMP for two times 90 min.[88] Fmoc removal was carried out with 20% piperidine in NMP for 70 s. Any remaining amino groups after incomplete coupling were acetylated by acetic anhydride/DIPEA/HOBt in NMP. After coupling of the final amino acid (Fmoc-Asp(OtBu)-OH), the Fmoc was removed and the resin was thoroughly washed with NMP and DCM, after which the peptide-resin was dried in a vacuum desiccator. The peptide was subsequently cleaved from the resin and deprotected by treatment with TFA/H_2O/1,2-ethanedithiol/triisopropylsilane (85:8.5:4.5:2, by vol.) for 3 h at room temperature. The peptide was precipitated at −20 °C with methyl tert-butyl ether/hexane (1:1, v/v). The precipitate was decanted, washed three times with cold methyl tert-butyl ether/hexane (1:1, v/v), and lyophilized from tert-butanol/H_2O (1:1, v/v).

For preparative HPLC runs, 50 mg of crude peptide was dissolved in 1 ml of TFA and 4 ml of buffer A (0.1% TFA in H_2O), loaded onto a Phenomenex Jupiter C4 column (250 mm × 22 mm, 10 μm particle size, 300 Å pore size), and eluted at a flow rate of 10 ml/min using a 80 min linear gradient from 100% buffer A to 100% buffer B (0.1% TFA in CH_3CN/H_2O (7:3, v/v)). Peptide purity was analyzed by analytical HPLC on a Phenomenex Jupiter C4 column (250 mm × 4.6 mm, 5 μm particle size, 300 Å pore size) at a flow rate of 1.0 ml/min using a 40 min linear gradient from 100% buffer A to 100% buffer B. A second HPLC analysis was performed with an Alltech Adsorbosphere XL C18 column (250 mm × 4.6 mm, 5 μm particle size, 300 Å pore size) at a flow rate of 0.75 ml/min using a 60 min linear gradient from 90% buffer C (0.1% TFA in H_2O/CH_3CN (8:2, v/v)) to 100% buffer D (0.1% TFA in CH_3CN/2-propanol/H_2O (50:45:5, by vol.)). Peptide purity was determined to be ≥95%. The peptide was characterized by mass spectrometry; the calculated average $(M+H)^+$ mass of the Aβ40 peptide is 4330.901, while values of 4330.642 and 4331.29 were found by MALDI-TOF and LC-ESI-MS, respectively.

Sample preparation

Aβ-lipid samples were prepared with the mixed film method that is commonly used to incorporate hydrophobic transmembrane peptides in lipid bilayers.[49] To dissolve any pre-existing aggregates of Aβ, the peptide was dissolved in 50 μl of TFA per milligram of peptide.[79] The excess of TFA was subsequently evaporated by a stream of nitrogen and the resulting peptide film was redissolved in 100 μl of TFE. This solution was mixed with 100 μl of a phospholipid solution in methanol/chloroform (1:1, v/v), followed by vortexing to ensure complete mixing of the peptide and lipid components. The resulting solution was completely clear. The solvents were evaporated by a stream of nitrogen or alternatively in a rotary evaporator, resulting in a transparent peptide-lipid film with a smooth appearance, which was dried overnight under high vacuum to remove residual solvent. For most experiments, the mixed film was hydrated, at a temperature above the main phase transition temperature of the lipids, with 1.2 ml of a buffer solution. EDTA was added to the buffers in order to avoid interactions of divalent metal ions with Aβ.[30,73] The hydrated proteoliposome suspension was freeze-thawed (five to ten cycles) to improve the size homogeneity of the multilamellar vesicles, and subsequent sample treatment depended on the technique used. The peptide and lipid concentrations also varied and are given below for the various measurements. Pure-lipid control samples were made in an identical way.

Circular dichroism

Mixed films with a 1:50 Aβ40/lipid molar ratio (containing 0.12 μmol of peptide) were prepared as described above and were hydrated with 1.2 ml of CD buffer (50 mM Tris-HCl (pH 7.4), 25 mM NaCl, 0.5 mM EDTA). After freeze-thawing, the samples were sonicated (~5 min, 25% duty cycle, 20% tip amplitude, output power

of 5 W) with a VCX750 sonicator equipped with a 6 mm diameter microtip (Sonics & Materials; Newtown, CT). The resulting suspension of unilamellar vesicles was centrifuged (1 h, 22,000*g*, 4 °C) to pellet titanium particles and any residual multilamellar vesicles or large Aβ aggregates. CD spectra of the clear supernatant fractions were recorded on a J-720 spectropolarimeter (Jasco International; Tokyo, Japan) equipped with a Haake C35/F8 water bath (1 mm path length cell, 0.5 nm data pitch, 1.0 s response time, 20 nm/min scan speed, 1 nm bandwidth). Spectra were corrected for the low-intensity CD signal of the lipids. For Aβ solubility assessment, 0.12 μmol of Aβ40 was dissolved in TFA and after evaporation of excess TFA, the Aβ film was solubilized or suspended in 1.2 ml of organic solvent. Samples with Aβ42 were prepared in the same manner, but contained only 12 nmol of peptide. CD spectra were recorded without any further sample manipulation, and were corrected for the spectral contribution of the various solvents. The secondary structure of Aβ was estimated by comparing the line shape and the intensity (residual molar ellipticity) of the experimental spectra with calculated reference spectra.[56]

Solid-state NMR spectroscopy

Dry films of pure POPC-d_{31} and mixed films of Aβ40/POPC-d_{31} with a 1:50 molar ratio (containing 0.5 μmol of peptide) were prepared as described above, but were dried from a total solvent volume of 6 ml before overnight exposure to high vacuum. Samples were hydrated with 3 ml of NMR buffer (50 mM Tris-HCl (pH 7.4), 150 mM NaCl, 1 mM EDTA) and the resulting suspension was repeatedly freeze-thawed. The multilamellar vesicles were either directly pelleted in a 5 mm silicon nitride rotor (Doty Scientific; Columbia, SC), or the vesicle suspension was sonicated and centrifuged (as described above) and either the pellet or the supernatant fraction were transferred to a rotor. Solid-state NMR measurements were performed on a Varian Inova 300 spectrometer (Varian; Palo Alto, CA) equipped with a 5-mm-diameter Doty Scientific magic angle spinning HXY probe, which was used in static mode at 23 °C. The operating frequencies were 46.09 MHz for ^{2}H and 121.55 MHz for ^{31}P, while ^{1}H decoupling was applied at 300.25 MHz. Broadline ^{1}H-decoupled ^{31}P NMR spectra were recorded (3.0 μs π/2 pulse, 2.0 s recycle delay, 60 kHz spectral width, 53 kHz ^{1}H decoupling) to characterize the macroscopic lipid organization. Typically 25,000 scans were acquired, and 2048 data points were used, with zero filling to 4096 points and an exponential multiplication resulting in a 100 Hz line broadening prior to Fourier transformation. ^{31}P NMR spectra were scaled to the same height and chemical shift was referenced to an aqueous solution of H_3PO_4 (85%). To assess the lipid acyl chain order, broadline ^{2}H NMR measurements were performed using a quadrupolar echo sequence (8.0 μs π/2 pulse, 40 and 30 μs pulse separations, 0.5 s recycle delay, 100 kHz spectral width, 4096 complex data points). Approximately 140,000 scans were accumulated. The free induction decays were left-shifted to begin at the top of echo and zero filled to 8192 points. For the supernatant fraction, ^{2}H NMR spectra were acquired with a one-pulse sequence (8.0 μs π/2 pulse, 1.0 s recycle delay, 100 kHz spectral width, 16,384 data points, 800 scans) and processed with zero filling to 32,768 points and a line broadening of 5 Hz. The ^{2}H chemical shift was referenced to $^{2}H_2O$.

Planar lipid bilayer recordings

Aβ channel-like activity was measured by fusion of Aβ40-containing unilamellar vesicles into a planar lipid bilayer. The vesicles also contained nystatin-ergosterol channels, which gradually deactivate after vesicle fusion, identifying individual vesicle fusion events.[63,64] Planar lipid bilayers were formed across a 150 μm aperture in the wall of a Delrin cup with a working volume of 1 ml (Warner Instruments; Hamden, CT). A small amount of a POPE/POPC (7:3 molar ratio) solution in *n*-decane (20 mg/ml) was applied to the area around the aperture and was allowed to air dry. The cup was placed in a bilayer chamber (Warner Instruments), the *cis* and *trans* chambers were filled with 1 ml of low-salt buffer (8 mM Hepes (pH 7.4), 150 mM NaCl, 1 mM EDTA), and a planar lipid bilayer was painted by depositing a small drop of the lipid-containing decane solution on the aperture. Formation and thinning of the bilayer were monitored by capacitance measurements; final capacitance values ranged from 70 to 100 pF. Subsequently, a 100 ml aliquot was removed from the *cis* chamber and replaced with 100 μl of a 3 M NaCl solution in distilled water and the chamber contents were carefully mixed. This procedure was repeated once with 100 μl and once with 50 μl of 3 M NaCl, giving a final *cis* chamber NaCl concentration of 720 mM. The *cis*/*trans* salt gradient facilitates vesicle fusion.

Mixed films were prepared with 15 nmol Aβ40, a peptide/lipid molar ratio of 1:200, and the lipid composition POPC/POPE/ergosterol (6:3:1 molar ratio). The film was hydrated with 1 ml of high-salt buffer (8 mM Hepes (pH 7.4), 720 mM NaCl) and the resulting suspension of multilamellar vesicles (7.5 mM total lipid) was freeze-thawed prior to extrusion through a polycarbonate filter to obtain unilamellar vesicles with a 400 nm diameter. These vesicles are estimated to contain about 8000 Aβ peptides each. To this suspension was added 50 μl of a bath sonicated solution of lyophilized nystatin in water-free methanol (1 mg/ml). The suspension was briefly bath sonicated and was left on the bench for 30 min, with occassional vortexing, to allow time for the nystatin (50 μg/ml) to interact with the vesicles and to form nystatin-ergosterol ion channels.[63] After this incubation, 10 μl of the vesicle suspension was added to the *cis* chamber, a holding potential of +100 mV was applied, with Ag/AgCl electrodes positioned in the *cis* and *trans* (virtual ground) chambers. The current signal, filtered at 1 kHz, was measured using a Bilayer Membrane Admittance Meter (model ID 562, Industrial Development Bangor; Gwynedd, UK). The signal was digitized with a BNC-2110 adapter and connected to a personal computer with a PCI-6014 data acquisition board (National Instruments; Austin, TX). Current data points were acquired at a rate of 2500 Hz and were saved using LabView software (National Instruments).

Atomic force microscopy

A suspension of unilamellar vesicles was prepared as described for the CD experiments, except that the total amount of Aβ40 in the mixed film was 16 nmol and that the film was hydrated with 1.25 ml of AFM buffer (50 mM Tris-HCl (pH 7.4), 150 mM NaCl, 1 mM EDTA). A 1 μl drop of this suspension was deposited on a freshly cleaved mica disk. The vesicles were allowed to adsorb to the mica for 15 h at a temperature of 4 °C. After extensive washing with AFM buffer and distilled water to remove non-adsorbed material, the mica disks were glued to

glass microscope slides and mounted on the scanner of a stand-alone MFP-3D AFM (Asylum Research; Santa Barbara, CA), with a closed loop in the *x*, *y* and *z* directions. Experiments were performed with silicon nitride Olympus TR800 cantilever tips with a nominal spring constant of 0.57 N/m (Olympus; Tokyo, Japan). Images were taken in alternate contact (AC) amplitude modulation mode in AFM buffer at an ambient temperature of 23 °C. Force curves were recorded of random areas of the samples, also in solution, with the same cantilever for all the samples. AC images of the samples were acquired before and after force curves were measured to ensure that the sample had not been damaged. The inverse optical lever sensitivity (nm/V) was calculated from force curves on mica. The sampling rate of the approach/retraction cycles was set to 200 nm/s. Only approach curves are shown. Samples were stored at 4 °C to prevent dehydration and were imaged again after two weeks.

ATR-FTIR spectroscopy

Mixed films with either a 1:50 or 1:25 Aβ40/lipid molar ratio (containing 0.80 μmol of lipid) were hydrated with 0.1 ml of a 0.1 M HCl solution and the resulting suspension was lyophilized overnight. This procedure replaces peptide-bound TFA molecules with HCl, preventing significant overlap of the TFA signal with the amide I bands from the peptide. The lyophilized sample was rehydrated with FTIR buffer (5 mM Hepes (pH 7.4), 25 mM NaCl) and freeze-thawed. This multilamellar vesicle suspension was either used directly for ATR-FTIR measurements, or was sonicated (~5 min, 25% duty cycle, output power of 25 W) using a Sonifier B-12 with a microtip (Branson Ultrasonics; Danbury, CT), and subsequently centrifuged (1 h, 16,000*g*, 4 °C) to obtain unilamellar vesicles. A 20 μl aliquot of multilamellar or unilamellar dispersion was spread on a germanium crystal plate (50 mm × 20 mm × 2 mm, Harrick EJ2121 (Harrick Scientific; Ossining, NY)) and excess water was removed with a nitrogen flow. The plates were placed under an aperture angle of 45°, yielding 25 internal reflections. ATR-FTIR spectra were recorded (2 cm^{-1} resolution, 128 scans, 800–4000 cm^{-1} range) at room temperature on a dry-air purged Bruker Equinox 55 FTIR spectrometer (Bruker Optics; Ettlingen, Germany) equipped with a mercury cadmium telluride detector. The spectral contribution of residual water vapor was subtracted using a scaling factor determined from the integrated absorbance of the 1555–1562 cm^{-1} bands.[89] Secondary-structure measurements were carried out on samples following deuteration for 1 h as described.[90] Briefly, Fourier self-deconvolution was applied to increase the resolution of the spectra in the amide I region. Least-squares iterative curve fitting was performed to fit different components of the amide I band revealed by the self-deconvolution to the non-deconvolved spectrum between 1700 and 1600 cm^{-1}. The proportion of various secondary structure elements was computed as reported.[90]

Acknowledgements

We thank Gabriel Mendes for electrical bilayer recordings and Fabrice Homblé for insightful discussion. This work was supported by the Biotechnology and Biological Sciences Research Council, the Engineering and Physical Sciences Research Council, the Medical Research Council, and the Ministry of Defence through the Bionanotechnology Interdisciplinary Research Collaboration. M.R.R.dP. was funded by the European Molecular Biology Organization. V.R. is Research Associate at the National Funds for Scientific Research (Belgium). F.S. acknowledges financial support from the Australian Research Council.

References

1. Wong, C. W., Quaranta, V. & Glenner, G. G. (1985). Neuritic plaques and cerebrovascular amyloid in Alzheimer disease are antigenically related. *Proc. Natl Acad. Sci. USA*, **82**, 8729–8732.
2. Mattson, M. P. (2004). Pathways towards and away from Alzheimer's disease. *Nature*, **430**, 631–639.
3. Hardy, J. A. & Higgins, G. A. (1992). Alzheimer's disease: the amyloid cascade hypothesis. *Science*, **256**, 184–185.
4. Lesné, S., Toh, M. T., Kotilinek, L., Kayed, R., Glabe, C. G., Yang, A. *et al.* (2006). A specific amyloid-β protein assembly in the brain impairs memory. *Nature*, **440**, 352–357.
5. Walsh, D. M., Klyubin, I., Fadeeva, J. V., Cullen, W. K., Anwyl, R., Wolfe, M. S. *et al.* (2002). Naturally secreted oligomers of amyloid β protein potently inhibit hippocampal long-term potentiation *in vivo*. *Nature*, **416**, 535–539.
6. Watson, D., Castaño, E., Kokjohn, T. A., Kuo, Y. M., Lyubchenko, Y., Pinsky, D. *et al.* (2005). Physicochemical characteristics of soluble oligomeric Aβ and their pathologic role in Alzheimer's disease. *Neurol. Res.* **27**, 869–881.
7. Esler, W. P. & Wolfe, M. S. (2001). A portrait of Alzheimer secretases - new features and familiar faces. *Science*, **293**, 1449–1454.
8. Marchesi, V. T. (2005). An alternative interpretation of the amyloid Aβ hypothesis with regard to the pathogenesis of Alzheimer's disease. *Proc. Natl Acad. Sci. USA*, **102**, 9093–9098.
9. Xu, Y., Shen, J., Luo, X., Zhu, W., Chen, K., Ma, J. & Jiang, H. (2005). Conformational transition of amyloid-β peptide. *Proc. Natl Acad. Sci. USA*, **102**, 5403–5407.
10. Mobley, D. L., Cox, D. L., Singh, R. R. P., Maddox, M. W. & Longo, M. L. (2004). Modeling amyloid β-peptide insertion into lipid bilayers. *Biophys. J.* **86**, 3585–3597.
11. Sengupta, P., Garai, K., Sahoo, B., Shi, Y., Callaway, D. J. E. & Maiti, S. (2003). The amyloid β peptide ($Aβ_{1-40}$) is thermodynamically soluble at physiological concentrations. *Biochemistry*, **42**, 10506–10513.
12. Terzi, E., Hölzemann, G. & Seelig, J. (1995). Self-association of β-amyloid peptide (1-40) in solution and binding to lipid membranes. *J. Mol. Biol.* **252**, 633–642.
13. Arimon, M., Díez-Pérez, I., Kogan, M. J., Durany, N., Giralt, E., Sanz, F. & Fernàndez-Busquets, X. (2005). Fine structure study of $Aβ_{1-42}$ fibrillogenesis with atomic force microscopy. *FASEB J.* **19**, 1344–1346.
14. Stine, W. B., Jr, Dahlgren, K. N., Krafft, G. A. & LaDu, M. J. (2003). *In vitro* characterization of conditions for amyloid-β peptide oligomerization and fibrillogenesis. *J. Biol. Chem.* **278**, 11612–11622.

15. Walsh, D. M., Klyubin, I., Fadeeva, J. V., Rowan, M. J. & Selkoe, D. J. (2002). Amyloid-β oligomers: their production, toxicity and therapeutic inhibition. *Biochem. Soc. Trans.* **30**, 552–557.
16. Petkova, A. T., Ishii, Y., Balbach, J. J., Antzutkin, O. N., Leapman, R. D., Delaglio, F. & Tycko, R. (2002). A structural model for Alzheimer's β-amyloid fibrils based on experimental constraints from solid state NMR. *Proc. Natl Acad. Sci. USA*, **99**, 16742–16747.
17. Lührs, T., Ritter, C., Adrian, M., Riek-Loher, D., Bohrmann, B., Döbeli, H. *et al.* (2005). 3D structure of Alzheimer's amyloid-β(1-42) fibrils. *Proc. Natl Acad. Sci. USA*, **102**, 17342–17347.
18. Chimon, S. & Ishii, Y. (2005). Capturing intermediate structures of Alzheimer's β-amyloid, Aβ(1-40), by solid-state NMR spectroscopy. *J. Am. Chem. Soc.* **127**, 13472–13473.
19. Huang, T. H. J., Yang, D. S., Plaskos, N. P., Go, S., Yip, C. M., Fraser, P. E. & Chakrabartty, A. (2000). Structural studies of soluble oligomers of the Alzheimer β-amyloid peptide. *J. Mol. Biol.* **297**, 73–87.
20. Georganopoulou, D. G., Chang, L., Nam, J. M., Thaxton, C. S., Mufson, E. J., Klein, W. L. & Mirkin, C. A. (2005). Nanoparticle-based detection in cerebral spinal fluid of a soluble pathogenic biomarker for Alzheimer's disease. *Proc. Natl Acad. Sci. USA*, **102**, 2273–2276.
21. Hortschansky, P., Schroeckh, V., Christopeit, T., Zandomeneghi, G. & Fändrich, M. (2005). The aggregation kinetics of Alzheimer's β-amyloid peptide is controlled by stochastic nucleation. *Protein Sci.* **14**, 1753–1759.
22. Harper, J. D. & Lansbury, P. T., Jr (1997). Models of amyloid seeding in Alzheimer's disease and scrapie: mechanistic truths and physiological consequences of the time-dependent solubility of amyloid proteins. *Annu. Rev. Biochem.* **66**, 385–407.
23. Alexandrescu, A. T. (2005). Amyloid accomplices and enforcers. *Protein Sci.* **14**, 1–12.
24. McLaurin, J., Yang, D.-S., Yip, C. M. & Fraser, P. E. (2000). Review: modulating factors in amyloid-β fibril formation. *J. Struct. Biol.* **130**, 259–270.
25. Gorbenko, G. P. & Kinnunen, P. K. J. (2006). The role of lipid-protein interactions in amyloid-type protein fibril formation. *Chem. Phys. Lipids*, **141**, 72–82.
26. LaFerla, F. M. (2002). Calcium dyshomeostasis and intracellular signalling in Alzheimer's disease. *Nature Rev. Neurosci.* **3**, 862–872.
27. McLaurin, J. & Chakrabartty, A. (1996). Membrane disruption by Alzheimer β-amyloid peptides mediated through specific binding to either phospholipids or gangliosides. *J. Biol. Chem.* **271**, 26482–26489.
28. McLaurin, J. & Chakrabartty, A. (1997). Characterization of the interactions of Alzheimer β-amyloid peptides with phospholipid membranes. *Eur. J. Biochem.* **245**, 355–363.
29. Terzi, E., Hölzemann, G. & Seelig, J. (1997). Interaction of Alzheimer β-amyloid peptide(1-40) with lipid membranes. *Biochemistry*, **36**, 14845–14852.
30. Curtain, C. C., Ali, F., Volitakis, I., Cherny, R. A., Norton, R. S., Beyreuther, K. *et al.* (2001). Alzheimer's disease amyloid-β binds copper and zinc to generate an allosterically ordered membrane-penetrating structure containing superoxide dismutase-like subunits. *J. Biol. Chem.* **276**, 20466–20473.
31. Gröbner, G., Glaubitz, G., Williamson, P. T. F., Hadingham, T. & Watts, A. (2001). Structural insight into the interaction of amyloid-β peptide with biological membranes by solid state NMR. In *Perspectives on Solid State NMR in Biology* (Kühne, S. R. & de Groot, H. J. M., eds), pp. 203–214, Kluwer Academic Publishers, Dordrecht.
32. Lindström, F., Bokvist, M., Sparrman, T. & Gröbner, G. (2002). Association of amyloid-β peptide with membrane surfaces monitored by solid-state NMR. *Phys. Chem. Chem. Phys.* **4**, 5524–5530.
33. Bokvist, M., Lindström, F., Watts, A. & Gröbner, G. (2004). Two types of Alzheimer's β-amyloid (1-40) peptide membrane interactions: aggregation preventing transmembrane anchoring *versus* accelerated surface fibril formation. *J. Mol. Biol.* **335**, 1039–1049.
34. Kremer, J. J., Pallitto, M. M., Sklansky, D. J. & Murphy, R. M. (2000). Correlation of β-amyloid aggregate size and hydrophobicity with decreased bilayer fluidity of model membranes. *Biochemistry*, **39**, 10309–10318.
35. Ege, C. & Lee, K. Y. C. (2004). Insertion of Alzheimer's Aβ40 peptide into lipid monolayers. *Biophys. J.* **87**, 1732–1740.
36. Maltseva, E., Kerth, A., Blume, A., Möhwald, H. & Brezesinski, G. (2005). Adsorption of amyloid β (1-40) peptide at phospholipid monolayers. *ChemBioChem*, **6**, 1817–1824.
37. Ege, C., Majewski, J., Wu, G., Kjaer, K. & Lee, K. Y. C. (2005). Templating effect of lipid membranes on Alzheimer's amyloid beta peptide. *ChemPhysChem*, **6**, 226–229.
38. Yip, C. M. & McLaurin, J. (2001). Amyloid-β peptide assembly: a critical step in fibrillogenesis and membrane disruption. *Biophys. J.* **80**, 1359–1371.
39. Alarcón, J. M., Brito, J. A., Hermosilla, T., Atwater, I., Mears, D. & Rojas, E. (2006). Ion channel formation by Alzheimer's disease amyloid β-peptide (Aβ40) in unilamellar liposomes is determined by anionic phospholipids. *Peptides*, **27**, 95–104.
40. Micelli, S., Meleleo, D., Picciarelli, V. & Gallucci, E. (2004). Effect of sterols on β-amyloid peptide (AβP 1-40) channel formation and their properties in planar lipid membranes. *Biophys. J.* **86**, 2231–2237.
41. Kourie, J. I., Henry, C. L. & Farrelly, P. (2001). Diversity of amyloid β protein fragment [1-40]-formed channels. *Cell. Mol. Neurobiol.* **21**, 255–284.
42. Arispe, N., Pollard, H. B. & Rojas, E. (1996). Zn^{2+} interaction with Alzheimer amyloid β protein calcium channels. *Proc. Natl Acad. Sci. USA*, **93**, 1710–1715.
43. Lin, H., Bhatia, R. & Lal, R. (2001). Amyloid β protein forms ion channels: implications for Alzheimer's disease pathophysiology. *FASEB J.* **15**, 2433–2444.
44. Lashuel, H. A., Hartley, D., Petre, B. M., Walz, T. & Lansbury, P. T., Jr (2002). Amyloid pores from pathogenic mutations. *Nature*, **418**, 291.
45. Quist, A., Doudevski, I., Lin, H., Azimova, R., Ng, D., Frangione, B. *et al.* (2005). Amyloid ion channels: a common structural link for protein-misfolding disease. *Proc. Natl Acad. Sci. USA*, **102**, 10427–10432.
46. Kayed, R., Sokolov, Y., Edmonds, B., McIntire, T. M., Milton, S. C., Hall, J. E. & Glabe, C. G. (2004). Permeabilization of lipid bilayers is a common conformation-dependent activity of soluble amyloid oligomers in protein misfolding diseases. *J. Biol. Chem.* **279**, 46363–46366.
47. Demuro, A., Mina, E., Kayed, R., Milton, S. C., Parker, I. & Glabe, C. G. (2005). Calcium dysregulation and membrane disruption as a ubiquitous neurotoxic mechanism of soluble amyloid oligomers. *J. Biol. Chem.* **280**, 17294–17300.
48. Dahlgren, K. N., Manelli, A. M., Stine, W. B., Jr, Baker, L. K., Krafft, G. A. & LaDu, M. J. (2002). Oligomeric

and fibrillic species of amyloid-β peptides differentially affect neuronal viability. *J. Biol. Chem.* **277**, 32046–32053.
49. de Planque, M. R. R., Goormaghtigh, E., Greathouse, D. V., Koeppe, R. E., 2nd, Kruijtzer, J. A. W., Liskamp, R. M. J. *et al.* (2001). Sensitivity of single membrane-spanning α-helical peptides to hydrophobic mismatch with a lipid bilayer: effects on backbone structure, orientation, and extent of membrane incorporation. *Biochemistry*, **40**, 5000–5010.
50. de Planque, M. R. R. & Killian, J. A. (2003). Protein-lipid interactions studied with designed transmembrane peptides: role of hydrophobic matching and interfacial anchoring. *Mol. Membr. Biol.* **20**, 271–284.
51. Arispe, N. (2004). Architecture of the Alzheimer's AβP ion channel pore. *J. Membr. Biol.* **197**, 33–48.
52. Townsend, M., Shankar, G. M., Mehta, T., Walsh, D. M. & Selkoe, D. J. (2006). Effects of secreted oligomers of amyloid β-protein on hippocampal synaptic plasticity: a potent role for trimers. *J. Physiol.* **572**, 477–492.
53. Cleary, J. P., Walsh, D. M., Hofmeister, J. J., Shankar, G. M., Kuskowski, M. A., Selkoe, D. J. & Ashe, K. H. (2005). Natural oligomers of the amyloid-β protein specifically disrupt cognitive function. *Nature Neurosci.* **8**, 79–84.
54. Marsh, D. (1990). *Handbook of Lipid Bilayers.* CRC Press, Boca Raton, FL.
55. Rainey, J. K. & Sykes, B. D. (2005). Optimizing oriented planar-supported lipid samples for solid-state protein NMR. *Biophys. J.* **89**, 2792–2805.
56. Greenfield, N. & Fasman, G. D. (1969). Computed circular dichroism spectra for the evaluation of protein conformation. *Biochemistry*, **8**, 4108–4116.
57. Seelig, J. (1978). ^{31}P nuclear magnetic resonance and the head group structure of phospholipids in membranes. *Biochim. Biophys. Acta*, **515**, 105–140.
58. Cullis, P. R. & de Kruijff, B. (1979). Lipid polymorphism and the functional roles of lipids in biological membranes. *Biochim. Biophys. Acta*, **559**, 399–420.
59. Davis, J. H. (1983). The description of membrane lipid conformation, order and dynamics by 2H-NMR. *Biochim. Biophys. Acta*, **737**, 117–171.
60. Separovic, F. & Gawrisch, K. (1996). Effect of unsaturation on the chain order of phosphatidylcholines in a dioleoylphosphatidylethanolamine matrix. *Biophys. J.* **71**, 274–282.
61. Petrache, H. I., Dodd, S. W. & Brown, M. F. (2000). Area per lipid and acyl length distributions in fluid phosphatidylcholines determined by ^{2}H NMR spectroscopy. *Biophys. J.* **79**, 3172–3192.
62. Lau, T. L., Ambroggio, E. E., Tew, D. J., Cappai, R., Masters, C. L., Fidelio, G. D. *et al.* (2006). Amyloid-β disruption of lipid membranes and the effect of metal ions. *J. Mol. Biol.* **356**, 759–770.
63. de Planque, M. R. R., Mendes, G. P., Zagnoni, M., Sandison, M. E., Fisher, K. H., Berry, R. M. *et al.* (2006). Controlled delivery of membrane proteins to artificial lipid bilayers by nystatin-ergosterol modulated vesicle fusion. *IEE Proc. Nanobiotechnol.* **153**, 21–30.
64. Woodbury, D. J. & Miller, C. (1990). Nystatin-induced liposome fusion. *Biophys. J.* **58**, 833–839.
65. Heinz, W. F. & Hoh, J. H. (1999). Spatially resolved force spectroscopy of biological surfaces using the atomic force microscope. *Trends Biotechnol.* **17**, 143–150.
66. Marra, J. & Israelachvili, J. (1985). Direct measurements of forces between phosphatidylcholine and phosphatidylethanolamine bilayers in aqueous electrolyte solutions. *Biochemistry*, **24**, 4608–4618.
67. Yip, C. M., Darabie, A. A. & McLaurin, J. (2002). Aβ42-peptide assembly on lipid bilayers. *J. Mol. Biol.* **318**, 97–107.
68. Fringeli, U. P. & Gunthard, H. H. (1981). Infrared membrane spectroscopy. *Mol. Biol. Biochem. Biophys.* **31**, 270–332.
69. Krimm, S. & Bandekar, J. (1986). Vibrational spectroscopy and conformation of peptides, polypeptides, and proteins. *Advan. Protein Chem.* **38**, 181–364.
70. Paul, C. & Axelsen, P. H. (2005). β sheet structure in amyloid β fibrils and vibrational dipolar coupling. *J. Am. Chem. Soc.* **127**, 5754–5755.
71. Matsuzaki, K. & Horikiri, C. (1999). Interactions of amyloid β-peptide (1-40) with ganglioside-containing membranes. *Biochemistry*, **38**, 4137–4142.
72. Kakio, A., Nishimoto, S., Yanagisawa, K., Kozutsumi, Y. & Matsuzaki, K. (2001). Cholesterol-dependent formation of GM1 ganglioside-bound amyloid β-protein, an endogenous seed for Alzheimer amyloid. *J. Biol. Chem.* **276**, 24985–24990.
73. Yoshiike, Y., Tanemura, K., Murayama, O., Akagi, T., Murayama, M., Sato, S. *et al.* (2001). New insights on how metals disrupt amyloid β-aggregation and their effects on amyloid-β cytotoxicity. *J. Biol. Chem.* **276**, 32293–32299.
74. Tashima, Y., Oe, R., Lee, S., Sugihara, G., Chambers, E. J., Takahashi, M. & Yamada, T. (2005). The effect of cholesterol and monoganglioside (GM1) on the release and aggregation of amyloid β-peptide from liposomes prepared from brain membrane-like lipids. *J. Biol. Chem.* **279**, 17587–17595.
75. Chromy, B. A., Nowak, R. J., Lambert, M. P., Viola, K. L., Chang, L., Velasco, P. T. *et al.* (2003). Self-assembly of $A\beta1_{-42}$ into globular neurotoxins. *Biochemistry*, **42**, 12749–12760.
76. Mastrangelo, I. A., Ahmed, M., Sato, T., Liu, W., Wang, C., Hough, P. & Smith, S. O. (2006). High-resolution atomic force microscopy of soluble Aβ42 oligomers. *J. Mol. Biol.* **358**, 106–119.
77. Bitan, G., Kirkitadze, M. D., Lomakin, A., Vollers, S. S., Benedek, G. B. & Teplow, D. B. (2003). Amyloid-β protein (Aβ) assembly: Aβ40 and Aβ42 oligomerize through distinct pathways. *Proc. Natl Acad. Sci. USA*, **100**, 330–335.
78. Chen, Y. R. & Glabe, C. G. (2006). Distinct early folding and aggregation properties of Alzheimer amyloid-β peptide Aβ40 and Aβ42: stable trimer or tetramer formation by Aβ42. *J. Biol. Chem.* **281**, 24414–24422.
79. Jao, S. M. K., Talafous, R., Orlando, R. & Zagorski, M. G. (1997). Trifluoroacetic acid pretreatment reproducibly disaggregates the amyloid β-peptide. *Amyloid Int. J. Exp. Clin. Invest.* **4**, 240–244.
80. Kagan, B. L., Azimov, R. & Azimova, R. (2004). Amyloid peptide channels. *J. Membr. Biol.* **202**, 1–10.
81. Hirakura, Y., Lin, M. C. & Kagan, B. L. (1999). Alzheimer amyloid Aβ1-42 channels: effects of solvent, pH, and Congo red. *J. Neurosci. Res.* **57**, 458–466.
82. Arispe, N., Pollard, H. B. & Rojas, E. (1993). Giant multilevel cation channels formed by Alzheimer disease amyloid-β protein [AβP-(1-40)] in bilayer membranes. *Proc. Natl Acad. Sci. USA*, **90**, 10573–10577.
83. Sato, H. & Feix, J. B. (2006). Peptide-membrane interactions and mechanisms of membrane destruction by amphipathic α-helical antimicrobial peptides. *Biochim. Biophys. Acta*, **1758**, 1245–1256.

84. Kayed, R., Head, E., Thompson, J. L., McIntire, T. M., Milton, S. C., Cotman, C. W. & Glabe, C. G. (2003). Common structure of soluble amyloid oligomers implies common mechanism of pathogenesis. *Science*, **300**, 486–489.
85. Fields, C. G., Lloyd, D. H., Macdonald, R. L., Otteson, K. M. & Noble, R. L. (1991). HBTU activation for automated Fmoc solid-phase peptide synthesis. *Peptide Res.* **4**, 95–101.
86. Wang, S. S. (1973). p-Alkoxybenzyl alcohol resin and p-alkoxybenzyloxycarbonylhydrazide resin for solid phase synthesis of protected peptide fragments. *J. Am. Chem. Soc.* **95**, 1328–1333.
87. Sieber, P. (1987). An improved method for anchoring of 9-fluorenylmethoxycarbonyl-amino acids to 4-alkoxybenzyl alcohol resins. *Tetrahedron Letters*, **28**, 6147–6150.
88. Tickler, A. K., Barrow, C. J. & Wade, J. D. (2001). Improved preparation of amyloid-β peptides using DBU as N^{α}-Fmoc deprotection reagent. *J. Peptide Sci.* **7**, 488–494.
89. Goormaghtigh, E., Raussens, V. & Ruysschaert, J.-M. (1999). Attenuated total reflection infrared spectroscopy of proteins and lipids in biological membranes. *Biochim. Biophys. Acta*, **1422**, 105–185.
90. Goormaghtigh, E., Cabiaux, V. & Ruysschaert, J.-M. (1990). Secondary structure and dosage of soluble and membrane proteins by attenuated total reflection Fourier-transform infrared spectroscopy on hydrated films. *Eur. J. Biochem.* **193**, 409–420.

Edited by F. E. Cohen

(Received 4 December 2006; received in revised form 19 January 2007; accepted 20 February 2007)
Available online 2 March 2007